AD-A054 851 MASSACHUSETTS INST OF TECH CAMBRIDGE DEPT OF AERONAU--ETC F/G 20/4
MODELING OF COHERENT STRUCTURE IN BOUNDARY LAYER TURBULENCE.(U)
1978 M T LANDAHL AFOSR-74-2730
UNCLASSIFIED AFOSR-TR-78-0962 NL

| OF |
AD
A054851

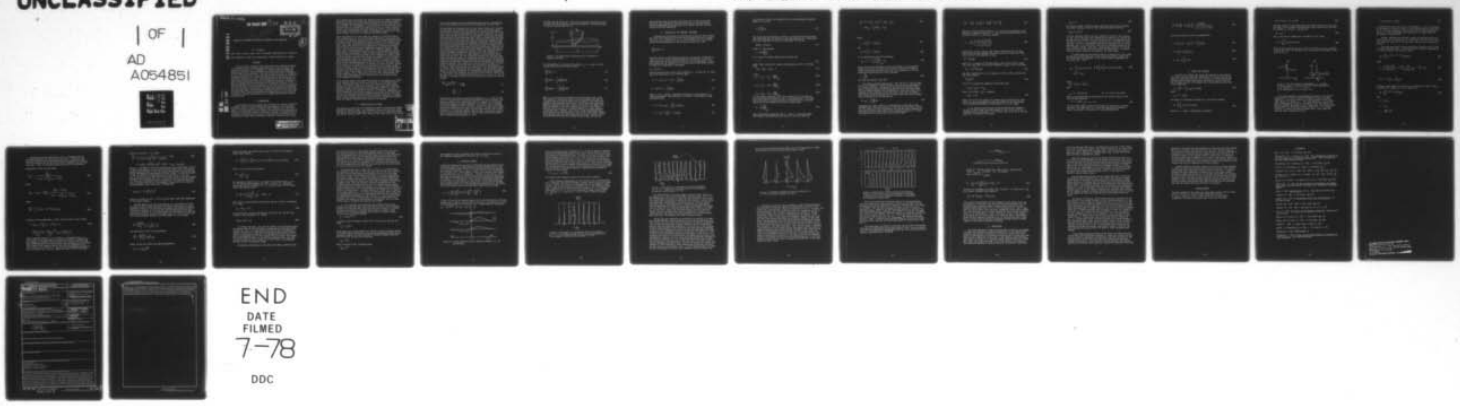

END
DATE
FILMED
7-78
DDC

MODELING OF COHERENT STRUCTURE IN BOUNDARY LAYER TURBULENCE

M. T. Landahl

Dept. Aero. & Astro., Mass. Inst. Technology, Cambridge, Mass. 02139 and

Dept. Mechanics, Royal Inst. Technology, S-10044 Stockholm 70, Sweden

ABSTRACT

The large-scale coherent motion associated with turbulent bursting in a boundary layer is studied with the aid of an inviscid model. The space-time evolution of a disturbance of large horizontal dimensions compared to the wall layer thickness is analyzed under the assumption that the mean flow is parallel. The initial velocity field is assumed to be set up by the action of the turbulent stresses produced by a patch of secondary instablity. For short and moderate times, the effects of viscosity and pressure are small, and the evolution of the disturbance is conveniently studied with the aid of Lagrangian techniques. The model is able to reproduce qualitatively many of the observed features of the bursting motion such as the formation of longitudinal streaks, the rapid acceleration after initiation of bursting, and the strong y-coherence of the u-fluctuations. In particular, the model demonstrates how action by the mean shear makes the disturbance eventually evolve into a thin internal shear layer, thus making possible the appearance of a new region of inflexional instability and hence burst regeneration-downstream of the original burst.

1. INTRODUCTION

The discovery of recent years that turbulence in the wall region of a boundary layer is highly intermittent and possesses a quasiperiodic and fairly distinct "bursty" structure (see Frenkiel et al. 1977 for a number of recent papers on this subject) has pointed to the necessity of analyzing in depth the dynamical processes involved in the generation of turbulent fluctuations in this region. This requires the adoption of a deterministic rather than a statistical approach since the usual statis-

tical methods are not suitable for dealing with such highly intermittent processes. Because the flows under consideration are extremely complicated undeady three-dimensional ones dominated by strong nonlinearity and rotation, the development of a successful theory necessitates a very careful choice of a theoretical model, one that it is simple enough to analyze, yet incorporates the major dynamical effects. Early such efforts emphasizing different aspects of the dynamics were those of Theodorsen (1952), Einstein & Li (1956) and Sternberg (1965).

Since turbulence may in some sense be regarded as a manifestation of flow instabilities, it is of considerable theoretical interest to try to relate the dynamical processes in the fully developed turbulent flow to those studied in hydrodynamic stability theory. This approach (Landahl, 1967, Bark, 1975) has proven partially successful in explaining some of the observed statistical properties of fluctuating pressures and velocities in terms of the propagation characteristics of linear waves. Later findings (Landahl, 1975, 1977) indicate, however, that other types of disturbances besides waves of the Tollmien-Schlichting type must be incorporated in order to model properly the fluctuation field. On basis of a two-scale model (first proposed in Landahl, 1973), in which the main nonlinear interaction was assumed to occur through a coupling between small and large scales of motion, it was concluded that large-scale motion in a localized region, a "coherent structure", would result from nonhomogeneous mixing in a patch of secondary instability of the inflectional type. In addition to waves of scales typical of the dimension of the patch, the large-scale eddy produced by the mixing will also contain a convected portion which will move downstream with the local mean velocity. The shearing of the convected eddy was found to lead to the formation of a new thin shear layer further downstream (Landahl, 1975), thus giving rise to a new inflectionally unstable region downstream of the original burst, and thereby making burst regeneration possible.

In the present paper a more detailed analysis of the dynamics of a large-scale coherent structure formed by the action of localized mixing is given. The approach taken is to treat the flow as an initial value problem with initial conditions provided by the large-scale momentum transfer caused by the mixing due to secondary instability. Since the processes involved are primarily inertial, viscosity is neglected. On the assumption that strong nonlinearity is primarily confined to the initial time period during the secondary instability phase, the evolution of each coherent structure could be analyzed separately, independently of other large-scale motion and statistical superposition used to model the random fluctuating flow field, if so desired.

2. FORMULATION OF THE MODEL

The theoretical model will be formulated on basis of the two-scale model proposed by Landahl (1973). The fundamental ideas underlying this model and some of the conclusions which can be drawn from it have been discussed earlier (Landahl, 1975, 1977). Here we shall only give a brief review

of its main features and draw some conclusions from it regarding the overall characteristics of the initial large-scale velocity field.

To understand the characteristics of the initial large-scale velocity field we must first discuss the behavior of the small-scale motion. The secondary instability giving rise to the small-scale motion is assumed to be of the Kelvin-Helmholtz type arising locally on a thin internal shear formed in the flow. The secondary instability, and hence the small-scale turbulence production, draws its energy from the velocity difference across the shear layer, and the resulting mixing will be such as to tend to remove the velocity difference (Landahl, 1975), The instability, and hence the turbulence production, will therefore eventually be quenched when the small-scale mixing has removed the local inflection in the large-scale velocity distribution. After an initial period of growth, the small-scale motion will therefore begin to decay slowly due to viscous dissipation. After the completion of the initial nonlinear growth phase, the motion will thus consist of a large-scale field on which is superimposed a slowly decaying small-scale velocity field, and the interaction between the large an small scales then becomes weak. The subsequent evolution of the large-scale velocity field may therefore be analyzed with the effects of the small-scale motion neglected. Furthermore, since the mechanisms involved are primarily inertial, the effects of viscosity may be omitted, at least during a moderate time period after the creation of the coherent structure. Since observed typical dimensions of the large-scale eddies are of the order the boundary layer thickness, the downstream rate of change of the mean properties of the boundary layer may be neglected in the analysis and therefore the parallel-flow assumption adopted for the mean flow. With disturbance velocities u_i ($u_1 = u$, $u_2 = v$, $u_3 = w$), pressure p, and mean velocity U(y) the equations of motion may thus be written

$$\frac{D(u_i + \delta_{1i}U(y))}{Dt} = -\frac{1}{\rho}\frac{\partial p}{\partial x_i} \tag{1}$$

$$\frac{\partial u_i}{\partial x_i} = 0 \tag{2}$$

The boundary conditions are that the component $u_2 = v$ is zero at the wall ($y = 0$) and that the disturbances vanish at large distances. The region occupied by the disturbance shall be assumed to be localized and have a typical horizontal dimension of ℓ, which will be assumed to be large compared to the thickness δ of the wall layer. Since the mean shear outside the wall and buffer regions is quite small compared to what it is inside this region, one may treat the mean flow in the wall layer as a separate boundary layer having a free-stream velocity equal to the value at the edge of the wall layer which may be taken to be located at approximately $y^+ = 50$.

Consider now the effect of a small-scale secondary instability occuring over a patch of typical horizontal dimension ℓ and confined within the wall region (see Fig. 1).

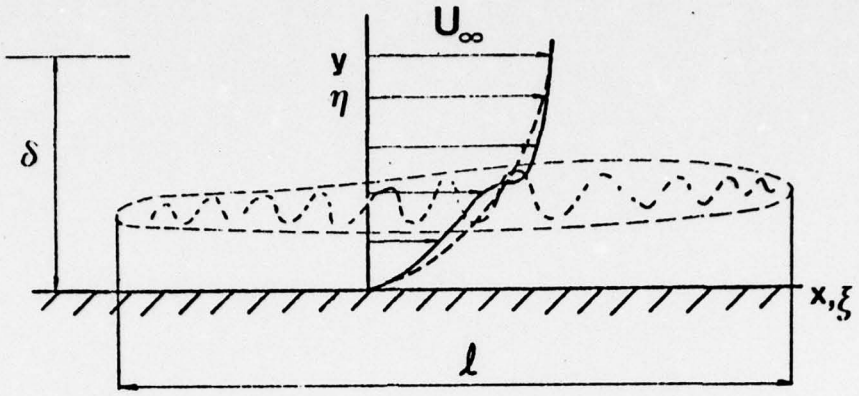

Figure 1. Two-scale model (conceptual) for initiation of coherent structure.

By integration of (1) and (2) over planes $x_2 = y = \text{const.}$ the following relations may be shown to hold:

$$\int_{-\infty}^{\infty}\int v\,dx\,dz = 0 \tag{3}$$

$$\int_{-\infty}^{\infty}\int x v\,dx\,dz = -\int_{t_i}^{t} dt \int_{-\infty}^{\infty}\int uv\,dx\,dz \tag{4}$$

$$\int_{\infty}^{\infty}\int x p_w\,dx\,dz = -\rho \int_{0}^{\infty} dy \int_{-\infty}^{\infty}\int uv\,dx\,dz \tag{5}$$

where t_i is the time of initiation of the disturbance and p_w the wall pressure. In deriving these it has been assumed that the disturbances drop off with distance from the center of the patch fast enough to make boundary terms vanish. A localized event producing Reynolds stresses of the usual sign ($\langle uv\rangle<0$) will thus impart a moment of momentum to the flow, through the action of the surfacd pressure, so as to give it a forward rotation in a sense opposite to the mean shear (Landahl, 1975, 1977). Large instantaneous Reynolds stresses are produced only as long as the small-scale instability persists; thus the right-hand side of (4) will receive its major contribution during the secondary growth stage, and the non-

linear effects from the small-scale motion will be small thereafter. Therefore, the subsequent evolution of the large-scale glow may be treated independently from the small-scale motion, and each coherent structure analyzed separately.

3. EVOLUTION OF THE COHERENT STRUCTURE

Following the discussions in the previous section we shall analyze the large-scale motion as an initial value problem with initial conditions u_o, v_o, w_o specified at $t_o = 0$ and selected so as to be commensurate with the properties of the secondary instability. Thus

$$\int_{-\infty}^{\infty}\int xv_o\,dxdz > 0$$

Also the initial u_o-distribution should be such that the streamwise velocity $(U + u_o)$ is free from reflections. (For simplicity, u_o will be taken to be zero in the numerical example to be treated below). A formal solution of the system (1), (2) is most easily constructed on basis of material ("Lagrangian") coordinates

$$\xi_i = (\xi,\eta,\zeta)$$

defining the position of each fluid element at $t = 0$ (see Fig. 1). From the first and third of (1) it follows that

$$u + U = u_o(\xi,\eta,\zeta) + U(\eta) - \frac{1}{\rho}\int_o^t p_x Dt_1 \tag{6}$$

$$w = w_o(\xi,\eta,\zeta) - \frac{1}{\rho}\int_o^t p_z Dt_1 \tag{7}$$

where $\int \dot{\sim} Dt_1$, denotes integration following a fluid element, i.e., holding ξ_i constant. The laboratory ("Eulerian") coordinates are then determined from

$$x = \xi + (U + u_o)t - \frac{1}{\rho}\int_o^t (t-t_1)p_x Dt_1 \tag{8}$$

$$z = \zeta + w_o t - \frac{1}{\rho}\int_o^t (t - t_1)p_z Dt_1 \tag{9}$$

The pressure is found by integration of the second momentum equation along x, z = const.,

$$p = \rho \int_y^\infty \frac{Dv}{Dt}\, dy \tag{10}$$

The second velocity component, finally, is found from the requirement that continuity must be satisfied. The transformation of a volume element from laboratory to material coordinates is given by

$$dxdydz = Jd\xi d\eta d\zeta \tag{11}$$

where J is the Jacobian

$$J = \det\left(\frac{\partial x_i}{\partial \xi_j}\right)$$

For a fluid of constant density we must have that

$$J = 1 \tag{12}$$

(Lamb, 1932, section 15). Hence, upon expansion of (12) it follows that

$$A_1 y_\xi + A_2 y_\eta + A_3 y_\zeta = 1 \tag{13}$$

where

$$A_1 = x_\zeta z_\eta - z_\zeta x_\eta \equiv \left(\frac{d\xi}{dy}\right)_{x,z} \tag{14a}$$

$$A_2 = x_\xi z_\zeta - x_\zeta z_\xi \equiv \left(\frac{d\eta}{dy}\right)_{x,z} \tag{14b}$$

$$A_3 = x_\eta z_\xi - x_\xi z_\eta \equiv \left(\frac{d\zeta}{dy}\right)_{x,z} \tag{14c}$$

The identities expressed in the last column of (14) are found by direct calculation setting dx = dz = 0 and making use of (13). One may easily solve (13) by the method of characteristics, or equivalently, by direct integration of (14 b), which gives

$$y = \int_0^\eta \frac{d\eta_1}{(A_2)_{x,z}} \tag{15}$$

where the boundary condition that y = 0 for η = 0 has been taken into account. By substituting (8) and (9) into (14 b) we find

$$A_2 = (1 + tu_{o\xi} - I_{1\xi})(1 + tw_{o\zeta} - I_{3\zeta}) \tag{16}$$

$$- (tu_{o\zeta} - I_{1\zeta})(tw_{o\xi} - I_{3\xi})$$

where

$$I_1 = \frac{1}{\rho} \int_o^t (t - t_1) p_x Dt_1 \tag{17}$$

and

$$I_3 = \frac{1}{\rho} \int_o^t (t - t_1) p_z Dt_1 \tag{18}$$

It is convenient to define the quantity

$$\ell_m \equiv y - \eta = \int_o^\eta \left(\frac{1-A_2}{A_2}\right)_{x,z} d\eta_1 \tag{19}$$

which gives the displacement of the fluid element in the direction normal to the wall, the quantity of primary interest in Prandtl's (1925) *mixing-length theory*. From this, the y-component of the perturbation velocity may be directly obtained

$$v = \frac{D\ell_m}{Dt} \tag{20}$$

and then the pressure from (10).

The formal solution given by (6) - (10) and (16) - (20) is exact within the framework of inviscid theory but can only be evaluated by an iterative procedure. Fortunately, the problem considered allows one to introduce some simplifying assumptions which make the evaluation much more tractable. The assumption of a large horizontal scale compared to the thickness of the wall layer allows one to neglect the pressure variation through the boundary layer (the usual boundary layer assumption) so that one may set

$$p \simeq p_\delta = \rho \int_\delta^\infty \frac{Dv}{Dt}\, dy \tag{21}$$

throughout the layer, where p_δ is the pressure at the edge of the boundary layer. The flow outside the layer may be taken to be irrational, provided the initial disturbance is such that fluid elements originating inside the shear layer do not penetrate outside $y = \delta$. From the equations for an irrational flow one finds that

$$\frac{p_\delta}{\rho} = -\left(\frac{\partial}{\partial t} + U_\infty \frac{\partial}{\partial x}\right)\Phi - \frac{1}{2}\left(\Phi_x^2 + \Phi_z^2 + v_\delta^2\right) \tag{22}$$

where U_∞ is the velocity outside $y = \delta$, Φ the velocity potential, and subscript δ denotes values at $y = \delta$. The velocity potential may be calculated in terms of v_δ from the integral

$$\Phi = -\frac{1}{2\pi}\iint_{-\infty}^{\infty} \frac{v_\delta(x_1, z_1, t)\, dx_1 dz_1}{\sqrt{(x-x_1)^2+(z-z_1)^2}} \tag{23}$$

Taking ℓ/U_∞ to be a typical time scale of evolution for the large-scale motion one may estimate the pressure to be of order (for times which are not large compared to ℓ/U_∞)

$$\frac{p}{\rho} = O(U_\infty v_0') \tag{24}$$

where v_0' is a measure of the amplitude of the initial motion. Using this, one finds that the pressure integrals I_1 and I_3 are of the order

$$I_{1,3} = O\left[t^2 U_\infty v_0'/\ell\right] \tag{25}$$

and their contribution to the integrand in (19) of order (taking only the linear terms)

$$t^2 U_\infty v_0'/\ell^2 \tag{26}$$

This will be negligible compared to the linear term

$$-\dot{t}(u_{0\xi} + w_{0\zeta}) = t\, v_{0n}$$

which is of order $t\, v_0'/\delta$, whenever

$$t\, U_\infty/\ell \ll \ell/\delta \tag{27}$$

Hence, for $\delta/\ell \ll 1$ the effects of pressure may be neglected for times which are not large compared to the time needed for the disturbance to be convected downstream a distance equal to its own length.

In the analysis which follows the perturbations are assumed to be small so that terms involving products of the initial velocity components may be neglected in the solution (19). From (16) it follows that this is permissible provided

$$v_o' t \ll \delta \tag{28}$$

For times of order δ/v_o' and larger, nonlinear selfdistortion effects may become important. Only for very weak disturbances such that

$$v_o'/U_\infty \ll (\delta/\ell)^2 \tag{29}$$

will the nonlinear effects be small compared to those of the pressure. If (29) is not satisfied, the solution may be obtained by iteration on the pressure as follows. First, the solution (19) is calculated by neglecting I, and I_3 in (16), Second, the pressure is obtained from (22) and (23), I_1 and I_3 are computed, and then an improved value of ℓm determined, etc. It is difficult to assess the convergence properties of such a method, however. Possibly, a step-by-step procedure in time in which after each time step a new initial velocity field is calculated could be used to study the flow behavior for large times.

To investigate the qualitative effects of pressure for large times, we have here instead made use of the linearized solution. Neglecting all terms which are quadratic in the initial velocity components we find from (10) - (19)

$$\ell_m = t \int_o^y v_{on}(\xi_1,\eta_1,z)d\eta_1 - \frac{1}{\rho} \nabla_2^2 \int_o^y dy \int_o^t (t-t_1)p(\xi_1,t_1,z)dt_1 \tag{30}$$

$$\equiv \ell_m^{(1)} + \Delta\ell_m$$

where

$$\nabla_2^2 = \partial^2/\partial x^2 + \partial^2/\partial z^2$$

and

$$\xi_1 = x - U(\eta_1)(t-t_1) \qquad (t_1 = 0 \text{ in the first term})$$

Here, use has been made of continuity of the initial velocity field and the approximations

$$x \simeq \xi + U(y)t \ , \ y \simeq \eta \ , \ z \simeq \zeta \tag{31}$$

The first term, $\ell_m^{(1)}$, in (30) may be regarded as the purely convected solution. The second term, $\Delta\ell$, gives the lowest-order correction due to the pressure. The pressure is now approximated by

$$\frac{p}{\rho} \simeq \frac{1}{2\pi}\left(\frac{\partial}{\partial t} + U_\infty \frac{\partial}{\partial x}\right) \iint_{-\infty}^{\infty} \frac{v_\delta \, dx_1 dz_1}{\sqrt{(x-x_1)^2 + (z-z_1)^2}} \tag{32}$$

and the perturbation velocity components by

$$u \simeq u_o(\xi,y,z) - \ell_m U'(y) - \frac{1}{\rho}\int_o^t p_x Dt_1 \tag{33}$$

$$v \simeq \left(\frac{\partial}{\partial t} + U_\infty \frac{\partial}{\partial x}\right) \ell_m \tag{34}$$

$$w \simeq w_o - \frac{1}{\rho}\int_o^t p_z \, Dt_1 \tag{35}$$

4. LARGE-TIME BEHAVIOR

We shall now consider the large-time behavior of the solution (19) under certain simplifying assumptions. It follows that for moderately large times such that (27) and (28) are satisfied both the pressure and nonlinear terms may be neglected in (19) so that the fluid element vertical displacement may be approximated by the linearized expression

$$\ell_m \equiv \ell_m^{(1)} = t\int_o^\eta v_{on}(\xi_1,\eta_1;z)d\eta_1 \tag{36}$$

where

$$\xi_1 = x - U(\eta_1)t$$

By change of integration variable to ξ_1 this may be written

$$\ell_m = \int_\xi^x \frac{1}{U_1'} v_{on}(\xi_1,\eta_1;z)d\xi_1 \tag{37}$$

where $\xi = x - U(y)t$ and where U_1' is given by

$$U_1 \equiv U(\eta_1) = (x - \xi_1)/t \tag{38}$$

Consider now $x/\ell \gg 1$ and large times (but within the limits set by (27) and (28)). Since sizeable contributions to the integral (37) come only for regions $\xi_1 = O(x/\ell)$, one may set

$$U_1 \simeq x/t \tag{39}$$

and η_1 may thus be replaced by a constant in (37) giving

$$\ell_m \simeq \frac{1}{U_1'} \int_{\xi}^{\infty} v_{o\eta}(\xi_1;\eta_1;z)d\eta_1 \tag{40}$$

where we have replaced the upper limit by infinity since $v_{o\eta}$ approaches zero for $x/\ell \gg 1$. The solution for ℓ_m will have the character illustrated in Fig. 2.

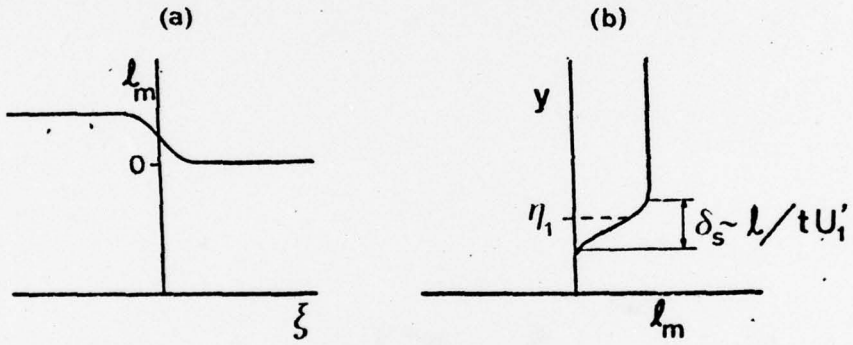

Figure 2. The fluid element displacement, ℓ_m , in the direction normal to the wall for large times (conceptual):
a) as function of $\xi = x - U(y)t$
b) as function of y. $U_1 \equiv U(\eta_1) = x/t$.

For large negative ξ (corresponding to large y) the range of integration will include the whole streamwise range of nonzero values of v_o, so that ℓ_m tends to a limiting nonzero value (provided $\int_{\eta}^{\infty} v_o d\xi \neq 0$) above $y = \eta$. For large positive ξ, on the other hand, (corresponding to small y) the lower limit will tend to $+\infty$ and the integral, and hence ℓ_m, will become zero. The fluid element displacement will hence vary rapidly, when $tU' \gg 1$, in a region around $y = \eta_1$ with a thickness of order $\ell/U't$. Since, when the pressure term is neglected in (33)

$$u \simeq u_o(\xi,y,z) - \ell_m U(y) \tag{41}$$

it follows that a thin shear layer, of thickness $\delta_s = \ell/U't$, decreasing as the inverse of time, will form. It also follows from the second term of (41) that the streamwise velocity will show a strong y-coherence for $y > \eta_1$. Such coherence has been observed in the experiments by Blackwelder & Kaplan (1976).

For the nonlinear case one must include the possibility that A_2 could become zero in some point for large times such that $v_o'/\delta = 0(\delta)$. The conditions under which this may arise have not been investigated, however.

The long-time effects of pressure may be studied on basis of the linearized equations (30) - (35). Application of Fourier transform in x, z and t to (30), (32) and (34), with

$$\hat{\ell}_m = \iiint_{-\infty}^{\infty} e^{-i(\alpha x + \beta z - \omega t)} \ell_m dx dz dt \tag{42}$$

gives

$$\hat{\ell}_m = \int_o^y \frac{v_{on}(\eta_1)d\eta_1}{[i\alpha(U_1-c)]^2} - k^2 \frac{\hat{p}}{\rho} \int_o^y \frac{d\eta_1}{[i\alpha(U_1-c)]^2} \equiv \hat{\ell}_m^{(1)} + \Delta\hat{\ell}_m \tag{43}$$

$$\frac{1}{\rho}\hat{p} = -\alpha^2(U_\infty - c)^2 \hat{\ell}_{m\delta}/k \tag{44}$$

In these, caret denotes triple Fourier transform as in (42), tilde a transform with respect to x and z, only, e.g.

$$\tilde{v}_o = \iint_{-\infty}^{\infty} e^{-i(\alpha x + \beta z)} v_o dx dz \tag{45}$$

and

$$U_1 = U(\eta_1)$$

$$c = \omega/\alpha$$

$$k = \sqrt{\alpha^2 + \beta^2}$$

The behavior of the solution for $\delta/\ell \ll 1$ is obtained from the transformed solution for small values of α and β . Similarly, the large-time behavior may be determined from the transform for small c. From the solutions for ℓ_m and p the velocity components may be found from (33) - (35), so only these quantitatives will be considered.

Combination of (43) and (44) gives

$$\hat{\ell}_{m\delta} = \frac{\hat{\ell}^{(1)}_{m\delta}}{1 + k(U_\infty - c)^2 \int_0^\delta (U_1 - c)^{-2} d\eta_1} \tag{46}$$

Hence,

$$\Delta\hat{\ell}_m = - k(U_\infty - c)^2 \hat{\ell}^{(1)}_{m\delta} \frac{\int_0^y (U_1 - c)^{-2} d\eta_1}{1 + k(U_\infty - c)^2 \int_0^\delta (U_1 - c)^{-2} d\eta_1} \tag{47}$$

where

$$\hat{\ell}^{(1)}_{m\delta} = \int_0^\delta [i\alpha(U_1 - c)]^{-2} \tilde{v}_0(\eta_1) d\eta_1 \tag{48}$$

Expansion of the denominator in (46), (57) for small c and k yields

$$1 + k(U_\infty - c)^2 \int_0^\delta (U_1 - c)^{-2} d\eta_1 \simeq 1 - \tag{49}$$

$$- \frac{k(U_\infty - c)\, U_\infty}{c\, U'_c} - \frac{k(U_\infty - c)^2}{U'^3_c} U''_c \ln\left(\frac{U_\infty - c}{-c}\right)$$

Index c denotes values at $\eta = \eta_c$, where η_c is defined by $U(\eta_c) = c$. That branch of the logarithm in the second term which is obtained by going below the integral must be chosen. This follows from the treatment of the problem as an initial-value one; convergence of the Fourier time integral then requires that αc has a positive imaginary part. (This difficulty is familiar in the theory of hydrodynamic instability for an inviscid flow, see Lin, 1955). For small k it is found that

(49) has a zero for $c = c_o$, where

$$\frac{c_o}{U_\infty} \simeq \frac{q}{1 + q\,[1 - U_\infty U_c'' (\pi i - \ln q)/U_c'^2]} + O(k^2) \qquad (50)$$

$$\simeq k\, U_\infty/U_c' + \pi i k^2 U_\infty^3\, U_c''/U_c'^4 + O(k^2) \equiv (c_{or} + i c_{oi})/U_\infty$$

where $q = k\, U_\infty/U_\infty'$. This gives the eigenvalue for an infinite wave train of (a small) wave number k in an inviscid parallel shear flow. (The approximation underlying (50) is the same as the one employed in the early analytical approaches to hydrodynamic stability theory. In fact the integral in (49) is identical to the integral K_1 in Lin, 1955 , p. 44). For $U_c'' > 0$, which will occur when the velocity profile has an inflection point somewhere, the imaginary part of c_o is positive and the waves will grow, i.e. the flow is unstable to small disturbances. The mean velocity profile of interest here has $U'' < 0$ everywhere, hence the flow is stable in the hydrodynamic sense. From (50) it follows that

$$c_{oi}/c_{or} \simeq \pi\, k\, U_\infty^2\, U_c''/U_c'^3 \qquad (51)$$

which is of order δ/ℓ for $k = O(1\ell)$ and thus small under the assumptions of the present theory.

For the study of the long-time behavior of a disturbance of large horizontal scale we need only retain the lowest-order terms in k and c, provided all poles in the transform are properly represented. By approximating the integrals in (47) and (48) through expansion of the integrand about the point y_c in the same manner as that employed in (49) and retaining only poles, but not logarithmic terms in c and U-c (which give rise to contributions varying as inverse powers of t), we obtain

$$\hat{\ell}_m \simeq \frac{\tilde{v}_{on}(\eta_c)}{\alpha^2\, U_c'} \frac{U}{(c - c_o)(U - c)} \qquad (52)$$

But from (43) we find in the same manner

$$\hat{\ell}_m^{(1)} \simeq \frac{\tilde{v}_{on}(\eta_c)}{\alpha^2\, U_c'} \frac{U}{c(U - c)} \qquad (53)$$

Hence, we may set, within the same approximation,

$$\hat{\ell}_m \simeq \frac{c}{c - c_o}\, \hat{\ell}_m^{(1)} \qquad (54)$$

After inversion, the results may be cast in form of the following convolution integral:

$$\ell_m = \frac{\partial^2}{\partial x \partial t} \int_0^t dt_1 \iint_{-\infty}^{\infty} G(x-x_1, z-z_1, t-t_1) \ell_m^{(1)}(x_1, y, z_1, t_1) dx_1 dz_1 \qquad (55)$$

where G is the inverse transform of

$$\hat{G} = \frac{1}{\alpha^2 (c - c_0)} \qquad (56)$$

An asymptotic analysis for $x, t \to \infty$ under the assumption that $c_{oi} < 0$ for all non-zero wave numbers, but that $|c_{oi}|/c_{or} \ll 1$ (which is consistent with the assumption $\delta/\ell \ll$, see (54), gives the following simple approximate result:

$$G = \frac{1}{\pi z} \sin \left[\frac{x z U_c'}{U_\infty (t U_\infty - x)} \right] \cdot H(t U_\infty - x) \qquad (57)$$

Here, H(x) is the Heaviside step function and $U_c' = U'(y_c)$ is defined by (c.f. (39))

$$U_c \equiv U(y_c) = x/t \qquad (58)$$

In deriving (57), use has been made of (the first of) (50) with the imaginary part neglected, i.e. taking

$$c_0/U_\infty \simeq q/(1 + q) \qquad (59)$$

It follows from (55), (57) that the effects of the pressure causes the leading edge of the disturbance to propagate with the free-stream velocity U_∞ . This is in accordance with the finding by Gustavsson (1978), in which it is shown that the continuous spectrum of the solution for a disturbance initiated in a boundary layer gives rise to a portion propagating with the free-stream velocity, both in the viscous and in the inviscid cases. It can also be shown from (55), (57) that ℓ_m tends to zero as t^{-2} or faster as $t \to \infty$ for fixed x, in accordance with the result of Gustavsson (1978).

Of possible significance is also that (57) shows a definite span-

wise periodicity with a wave length increasing with time. This will also cause a cut-off for the larger spanwise scales, so that they tend to propagate with a lower velocity ($tU_\infty - x$ larger) than those with small spanwise scales. That the highest propagation velocities are attained by the disturbances of the smallest spanwise scales is a consequence of the form of the approximate dispersion relation (50). This was derived under the assumption of a large horizontal scale, so that the propagation velocities near U_∞ predicted for the small scales are not correctly given by this theory.

An interesting limit is that for $t \to \infty$ with $x/t = U_c$ held fixed. The argument of the sine in (57) then tends to a fixed value, and one can show that ℓ_m approaches a nonvanishing value for $t \to \infty$, provided $U(y) < U_c < U_\infty$. Hence, the streamwise dimension of the disturbed region will grow as $t(U_\infty - U(y))$. Since the largest differences between the free tream velocity and the local mean velocity $U(y)$ are found near the wall, one would thus expect the most highly elongated disturbances to appear there. This may provide a possible explanation for the streaky structure observed to occur in the turbulent boundary layer in the region close to the wall. However, in a real viscous flow the pressure cannot give rise to nondecaying disturbances, unless neutrally stable or growing waves are present because of instability. In the inviscid case, waves of $\alpha \to 0$ will always be nondecaying, even if the flow is hydrodynamically stable, and they provide the main contributions to the nondecaying disturbances in the limit of $t \to \infty$. In the viscous case, the waves with $\alpha \to 0$ will be decaying, and the disturbed region will therefore not continue to grow forever, but decay will set in at some finite value of streamwise to spanwise wave length.

It is of interest to estimate the time required for viscous effects to become important. By comparing the rate at which viscosity diffuses the internal shear layer with the rate at which it is being thinned by stretching of spanwise mean vorticity, Landahl (1977) arrived at the following estimate of the time t_v at which viscous diffusion and stretching balance:

$$t_v \sim (\ell^2/\nu U'^2)^{1/3} \tag{60}$$

In terms of wall variables, taking for U' the value at the wall one finds

$$t_v^+ \sim (\ell^+)^{2/3}$$

which shows that viscous effects are likely to become important before the disturbance has travelled a distance downstream many times its own streamwise length. The time required for viscous diffusion from the wall to be felt in the flow is given by

$$t_{vw} \sim y^2/\nu$$

which in terms of wall variables gives

$$t_{vw}^+ \sim y^{+2}$$

which appears to give a somewhat less severe restriction, except in the immediate neighborhood of the wall ($y^+ < 5$, say).

5. NUMERICAL EXAMPLE

A numerical example will be used to illustrate the application of the simplified model and a comparison made with experimental data. From (3) it follows that the initial v-distribution must be such that the net vertical flow across a plane y = const. must be zero. According to (4) the moment of v_o with respect to the z-axis should on the average be positive, since $\langle uv \rangle$ is negative, typical v_o-distribution will thus have values that are positive downstream and negative upstream of the center of the disturbance. Also, since the Reynolds stresses drop to zero for $y = 0$ and for $y = \delta$, the initial v-distribution must be zero in these limits and have a maximum near the position of maximum turbulence production. For the calculations presented here, the following v_o-distribution which satisfied these conditions was chosen:

$$v_o = C_o \left(\frac{x^+}{\ell_1^+}\right) \left(\frac{y^{+2}}{\ell_2^+}\right) \exp\left[-\left(\frac{x^+}{\ell_1^+}\right)^2 - \left(\frac{y^+}{\ell_2^+}\right)^2\right] \tag{61}$$

In this, ℓ_1^+ and ℓ_2^+ are scaling factors to be suitably selected. The plus superscript is used to indicate that viscous wall variables will be used in the presentation of the results. Fig. 3 shows numerical values for $C_o = \sqrt{2}\, e^{3/2}$, $\ell_1^+ \simeq 50$ and $\ell_2^+ = 16$

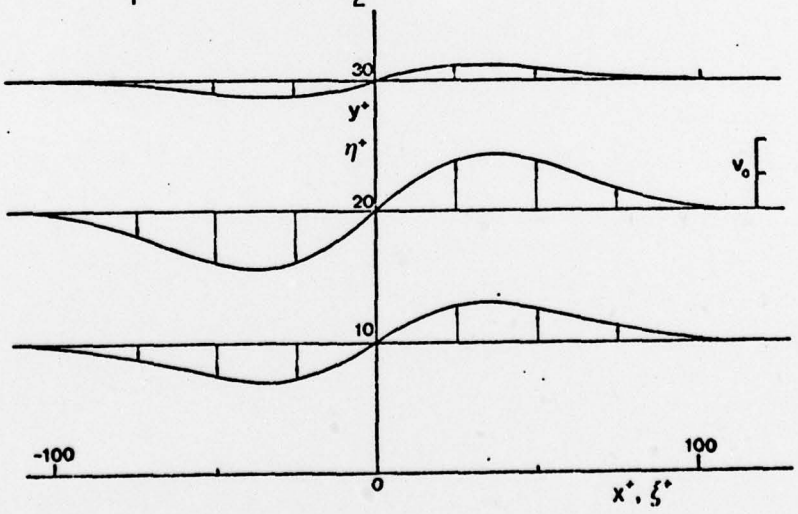

Figure 3. Initial condition used in numerical example $u_o = 0$, v_o from (61).

This v_0-distribution has a maximum at $y^+ = 16$ and an overall streamwise dimension of approximately 200 in wall units, values which are not inconsistent with experimental data. The value of C_0 was selected to make the maximum of v_0 equal to unity (i.e. equal to the wall friction velocity in dimensional form). At $y^+ = 40$, v_0 is about 0.03 and hence of negligible magnitude above this y^+-value. The character of the solution depends primarily on the scaling factor ℓ_2^+; by a simple linear rescaling the results for a given parameter combination may be applied to any other desired combination of C_0 and ℓ_1^+. For a representation of the mean velocity distribution the simple exponential approximation proposed by Schubert & Corcos (1965)

$$U^+ = 16\,(1 - e^{-y^+/16}) \tag{62}$$

was found to give adequate accuracy for the present purpose.

Fluid element displacements ℓ_m, and from this the u-perturbations, were calculated with pressure effects ignored. Sample results are shown in Fig. 4 and 5. At first, the streamwise velocity perturbation grows rapidly, and the flow pattern is stretched out in the streamwise direction. A shear layer is seen to form and intensify as it is convected downstream. For $t^+ = 5$ it is just beginning to appear between about $x^+ = -50$ and $x^+ = 0$, and for $t^+ = 15$ it is most intense at around $x^+ \simeq 50$.

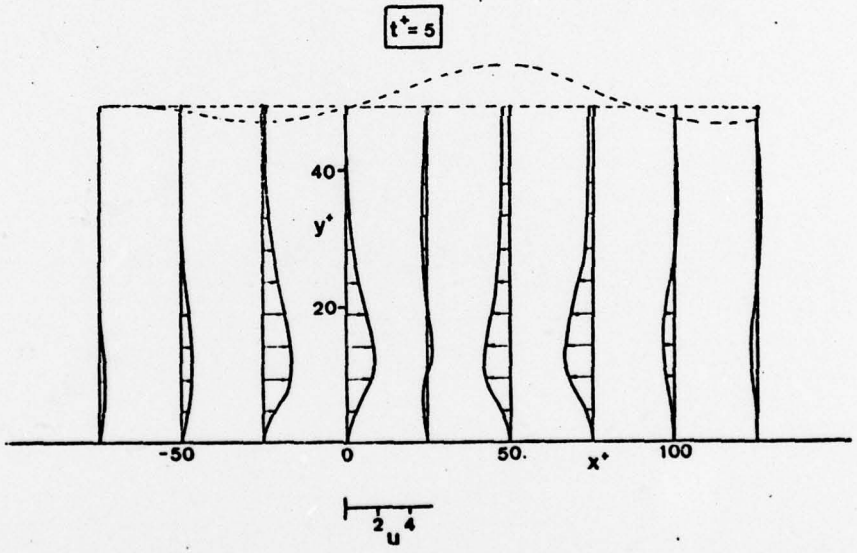

Figure 4. Distribution of streamwise velocity perturbation u at $t^+ = 5$ for model example. Dotted line gives position of fluid elements originally located along $y^+ = 50$.

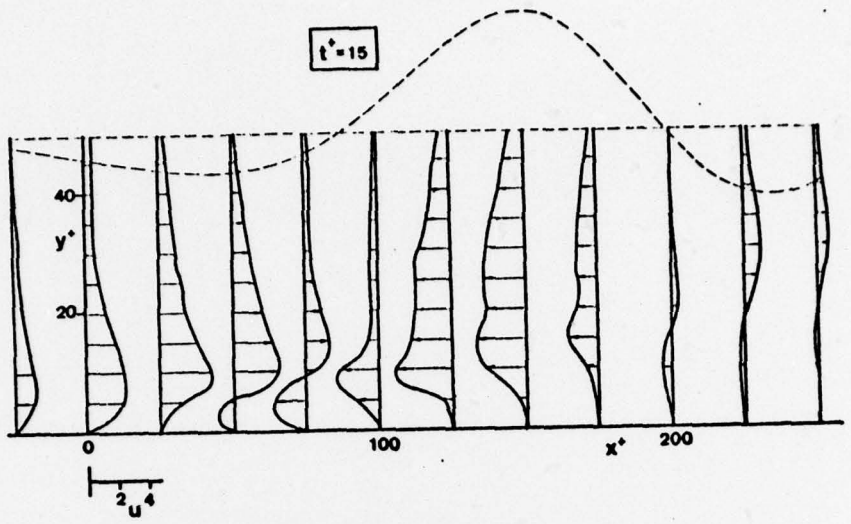

Figure 5. Distribution of streamwise velocity perturbation at $t^+ = 15$. Dotted line gives position of fluid elements originally located along $y^+ = 50$.

The displacement of the outer edge of the wall layer (taken to be located at $y^+ = 50$) is also indicated in both figures. For $t^+ = 15$ the displacement has become so large that the validity of the linearized theory may be seriously in doubt for this choice of initital velocity amplitudes. Nevertheless, the characteristic features shown by the theory such as the appearance of a bulge next to a depression further downstream are likely to be correctly represented. The depression and bulge will be convected downstream with a velocity less than U_∞, and the fluid riding over the outer edge of the wall layer will induce a pressure pattern which could be expected to consist of an overpressure in the region below the depression and an underpressure below the bulge. This pattern will then disperse as waves.

Perhaps the most revealing way to present the results is to show how the perturbation velocity distribution at a given downstream location varies with time. This would be what would be seen in experiments such as those of Blackwelder & Kaplan (1976) in which instantaneous velocity distributions were measured by a hot-wire rake. The variable-interval time-averaging (VITA) detection and sampling method employed by them could be expected to pick out structures which have formed just upstream of the measurement station. Accordingly, the station $x^+ = 50$, a position about half-way downstream of the center of the initial disturbance, was chosen as one which might correspond qualitatively to the experimental situation. In Fig. 6 are shown the streamwise perturbation velocities as function of y^+ at various nondimensional time t^+ after the initiation of the disturbance. One sees first a velocity defect extending throughout the whole layer. This arises because the station considered is first affected by fluid elements which have been lifted up by the initial v_0-distribution. At $t^+ = 10$ the regions further out from the wall have begun to receive fluid elements travelling towards the

wall, and an accelerated region begins to fill up the whole y^+ -range. The perturbation velocities then decay slowly to zero.

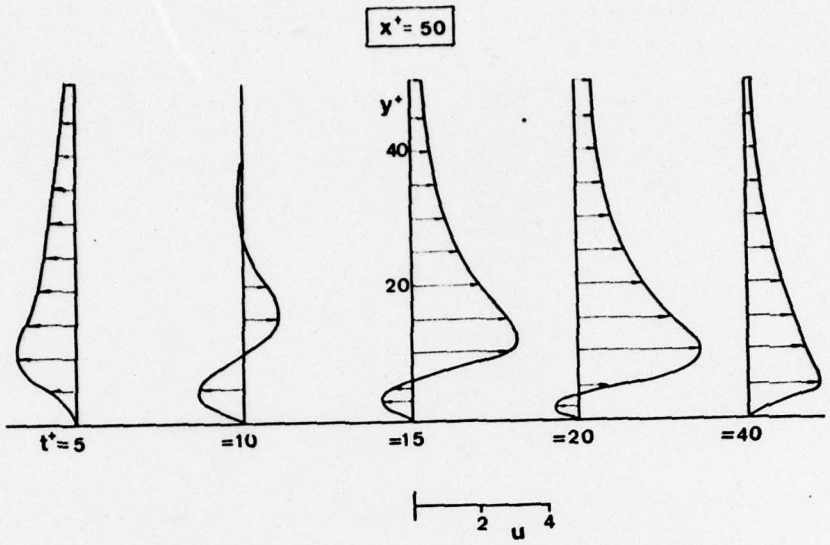

Figure 6. Streamwise perturbation velocity profile for $x^+ = 50$ at various instances of time.

The model calculations may be compared to the conditionally sampled perturbation velocities obtained by Blackvelder & Kaplan (1972) using their VITA procedure. These are reproduced in Fig. 7. As seen, the results obtained from the theoretical model are remarkably similar to the experimental ones. The most characteristic features of the measured data, which are correctly represented by the theory, is the strong shear layer, which appears to propagate towards the wall, and the very rapid acceleration associated with the passage of the shear layer. The experiments also show the predicted slow deceleration back to the undisturbed mean flow. The main qualitative difference is the observed excess velocity in the outer layer for early times which is not included in the simplified model. This velocity excess is probably a manifestation of the wallward motion (the sweep) which has been observed to precede the bursting (Corino & Brodkey, 1969 Offen & Kline, 1974) and which appears to be essential for the initiation of the lift-up and subsequent break-up of the flow in the wall region. This sweep is believed to originate in a previous burst further upstream. Since it was assumed for the initial conditions that $u_0 = 0$, the calculated results will show small streamwise perturbations in the outer region for small times.

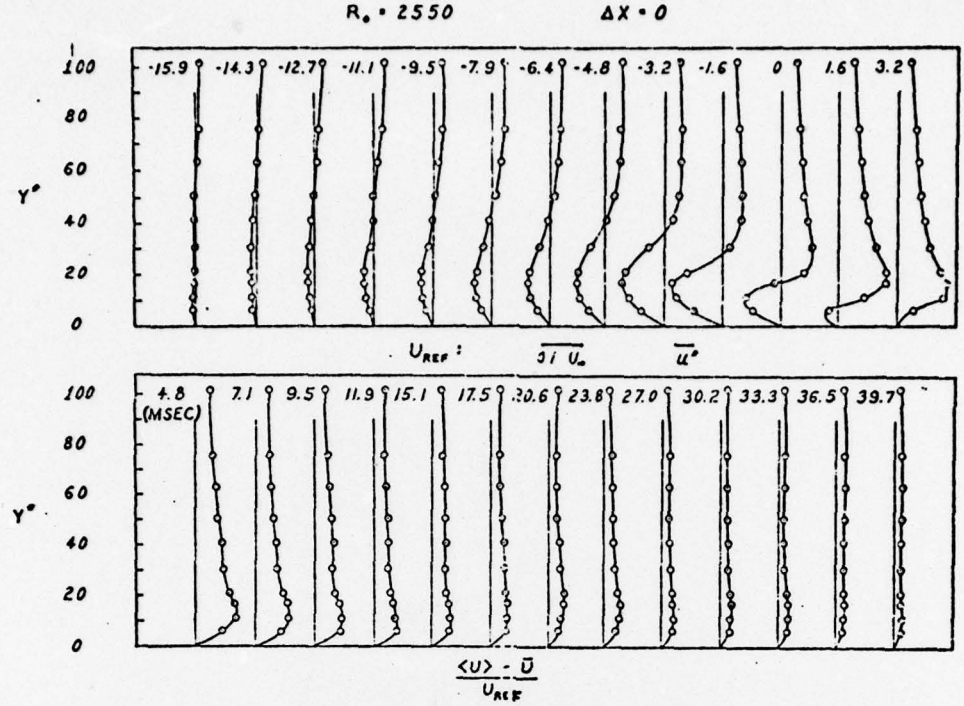

Figure 7. Conditionally (VITA) averaged u-perturbation velocity profiles with positive and negative time delay τ relative to the time of detection obtained in experiments by Blackwelder & Kaplan [29].

The sign predicted by the present theory for the perturbation velocity in the outer region caused by an earlier upstream burst may be determined from the approximate asymptotic solution (40). For values of y greater than the value $y_{|v_o|max}$ for which v_o has its largest magnitude, v_{on} is negative for the downstream region in ξ and positive for the upstream region. Therefore, the integral in (40) will be negative, and the fluid elements therefore tend to be displaced towards the wall in this region (see Fig. 8), i.e. a velocity excess occurs. For the region closer to the wall, for $y<y_{|v_o|max}$, the opposite situation prevails. Thus, a velocity excess tends to develop in the outer region for large times, and this may travel downstream to interact with a new burst.

For large times the effects of pressure must be taken into account, which may be accomplished through application of (55). By substituting into (57) the exponential approximation (62) for the velocity profile, G becomes, expressed in wall variables

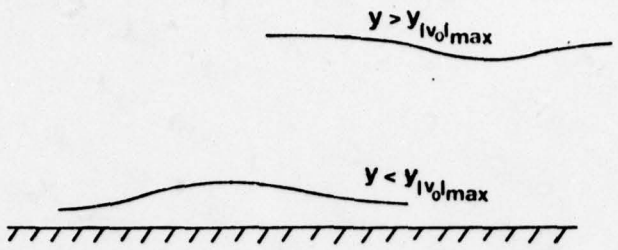

Figure 8. Typical streak lines. Upper curve, y greater than value $y_{|v_0|max}$ for which $|v_0|$ is maximum. Lower curve, $y < y_{|v_0|max}$.

$$G^+ = \frac{1}{\pi z^+} \sin\left[\frac{x^+ z^+}{U_\infty^+ \, t^+ \delta^+}\right] H\,(t^+ U_\infty^+ - x^+) \tag{63}$$

in which, in accordance with (62), $U_\infty^+ = 16$ and $\delta^+ = 16$. With $x^+/t^+ = U_c^+$. this gives a spanwise wave length of

$$\lambda_z^+ = 2\pi\delta^+ \, U_\infty^+ / U_c^+ \simeq 100 \, U_\infty / U_c \tag{64}$$

Since initial disturbances of finite spanwise scales always give rise to propagation velocities less than the free-stream velocity, this expression gives a somewhat larger spanwise streak spacing than the accepted experimental value of $\lambda_z^+ \simeq 100$ (see Gupta et al., 1971). However, for such a small scale the basic assumption of the theory, namely that the horizontal scale is large compared to the thickness of the wall layer, is of questionable validity. Even more serious is the neglect of viscosity for this case, since it is likely to have a considerable effect on the dispersion characteristics of the pressure waves. Therefore, the fairly good quantitative agreement between theory and experiments in this case is probably fortuitous.

6. CONCLUSIONS

The simple theoretical model presented here is based on the assumption that the interaction mechanism responsible for the generation of turbulent fluctuations is basically inviscid and involves the interaction of eddy motion of two disparate length scales, a large-scale one, typically of a dimension of the order of the boundary layer thickness, and a small-scale one, of a dimension smaller than the thickness of the wall layer. The large-scale eddy is set into motion by the action of the nonuniform Reynolds stresses produced by inflectional instability

of a thin internal shear layer. The turbulent mixing due to this instability can be shown to induce a slow forward rotation of the large-scale flow, in a sense opposite to the mean shear. That bursting regions indeed show such a rotation has recently been found in pipe-flow experiments by Sabot & Comte-Bellot (1976).

Under the assumption that the horizontal dimensions of the large-scale field are large compared to the thickness of the wall layer it can be shown that the effects of pressure and of nonlinearity on the evolution of the large-scale eddy may be neglected during short and moderate times after its initiation. By use of a Lagrangian analysis a simple formula for the displacement of the fluid element in the direction normal to the wall could then be derived. From this, one may then easily calculate the streamwise perturbation velocity in the spirit of Prandtl's mixing-length theory.

From the approximate theory one can demonstrate that a localized disturbance tends to develop into a thin shear layer during its downstream travel. A numerical example presented to illustrate the theory shows clearly this tendency and also gives qualitative agreement with conditionally averaged data obtained in the experiments by Blackwelder & Kaplan (1972). For large times after the intitiation of the disturbance, measured in terms of the time it requires to be convected downstream a distance equal to its own length, nonlinearity, pressure, and viscosity may all become important. Nonlinear effects may be handled fairly easily by the theory for cases for which the pressure gradient effects are small.

The effects of pressure, which provide the most intricate part of the analysis, were studied on basis of the linearized equations. It was found that for large times the pressure waves will give rise to an elongated pattern whose streamwise length will continue to grow as the long waves become more and more dominant. The flow will thus become increasingly two-dimensional in planes normal to the x-axis within this pattern. From (30) it therefore follows that the pressure effect will depend primarily on p_{zz}. At a spanwise pressure maximum, p_{zz} will be negative, and the contribution to ℓ_m will be negative, i.e., the flow will be speeded up. The opposite will be true for a pressure minimum. Since a region of $p_{zz} < 0$ must always have neighboring spanwise regions of $p_{zz} > 0$, a high-speed streak could be expected to be located between two low-speed streaks. That low-speed streaks tend to occur in pairs is consistent with observations of the streaky structure in the viscous sublayer (see Gupta et al., 1971). The present theory also gives an estimate of the spacing between longitudinal streaks in terms of the wave propagation characteristics for waves of large streamwise wave lengths.

It has been proposed by Offen & Kline (1975) and others that the inflectional region preceding breakdown is caused by a large-scale travelling pressure disturbance, originating in the outer portions of the boundary layer, which will retard the fluid elements near the wall through the action of a local adverse pressure gradient. Measurements reported by Willmarth (1975) show that intermittent Reynolds stress pro-

duction is associated with the passage of a large-scale pressure minimum which would indicate that the fluid near the wall, having a velocity less than the convection velocity of the pressure, had been subjected to retardation by a positive pressure gradient just before bursting. An estimate on basis of the present inviscid theory gives, in contrast, that this effect tends asymptotically to zero as the time of travel of the disturbance tends to infinity. The result of the present theory that a large lift-up would occur at a spanwise minimum of the pressure is not inconsistent with the experimental findings, however.

Simple estimates show that viscosity is likely to become important at about the same time pressure effects begin to be felt. From comparisons between the viscous and inviscid stability analysis, it could be expected that the propagation characteristics of the waves induced during the large-scale motion will be changed considerably by viscosity. An initial-value analysis similar to the one carried out here but with viscosity taken into account would therefore be desirable. Some initial efforts in this direction have been made by Gustavsson (1978) but the analysis becomes considerably more complicated than the one presented here and the results much more difficult to interpret.

ACKNOWLEDGEMENT

The work reported in this paper was supported in part by the Air Force Office of Scientific Research under Grant AFOSR 74-2730.
My special thanks go to Mrs. Gunnel Nordenfelt and Mrs. Ingrid Pramberg for an expert typing job under trying circumstances .

REFERENCES

Bark, F.H. 1975 J. Fluid Mech. 70, 229

Blackwelder, R.F. & Kaplan, R.E. 1972 "The intermittent Structure of the Wall Region of a Turbulent Boundary Layer" Paper presented at the 13th IUTAM Congress, Moscow

Blackwelder, R.F. & Kaplan, R.E. 1976 J. Fluid Mech. 76, 89

Corino, E.R. & Brodkey, R.S. 1969 J. Fluid Mech. 37, 1

Einstein, H.A. & Li, H. 1956 Proc. ASCE, J. Eng. Mech. Div. 82, EM 2

Frenkiel, N.F., Landahl, M.T. & Lumley, J.L. 1977 Phys. Fluids, 20, No. 10, Pt. II

Gupta, A.K., Laufer, J. & Kaplan, R.E. 1971 J. Fluid Mech. 50, 493

Gustavsson, L.H. 1978 On the evolution of disturbances in boundary layer flows, TRITA-MEK-78-02, The Royal Inst. Technology, Stockholm, Sweden

Lamb, H. 1932 Hydrodynamics, 6th ed., Cambridge University Press

Landahl, M.T. 1967 J. Fluid Mech. 29, 441

Landahl, M.T. 1973 in Proceedings of the 13th IUTAM Congress, 177 Springer Verlag

Landahl, M.T. 1975 SIAM, J. Appl. Math. 28, 735

Landahl, M.T. 1977 Phys. Fluids 20, No. 10, Pt. II, S55

Lin, C.C. 1955 The Theory of hydrodynamics Stability, Cambridge University Press

Offen, G.R. & Kline, S.J. 1974 J. Fluid Mech. 62, 233

Offen, G.R. & Kline, S.J. 1975 J. Fluid Mech. 70, 209

Prandtl, L. 1925 Z. angew. Math. u. Mech. 5, 136

Sabot, J. & Comte-Bellot, G. 1976 J. Fluid Mech. 74, 767

Sternberg, J. 1965 AGARD-ograph 97

Theodorsen, T. 1952 in Proc. of the Second Midwestern Conference of Fluid Mechanics, Ohio State University

AIR FORCE OFFICE OF SCIENTIFIC RESEARCH (AFSC)
NOTICE OF TRANSMITTAL TO DDC
This technical report has been reviewed and is approved for public release IAW AFR 190-12 (7b).
Distribution is unlimited.
A. D. BLOSE
Technical Information Officer

UNCLASSIFIED

SECURITY CLASSIFICATION OF THIS PAGE (When Data Entered)

(18) (19) REPORT DOCUMENTATION PAGE		READ INSTRUCTIONS BEFORE COMPLETING FORM
1. REPORT NUMBER AFOSR-TR-78-0962 ✓	2. GOVT ACCESSION NO.	3. RECIPIENT'S CATALOG NUMBER
(6) 4. TITLE (and Subtitle) MODELING OF COHERENT STRUCTURE IN BOUNDARY LAYER TURBULENCE. ✓		5. TYPE OF REPORT & PERIOD COVERED (9) INTERIM rept., 6. PERFORMING ORG. REPORT NUMBER
(10) 7. AUTHOR(s) M. T. LANDAHL	(15)	8. CONTRACT OR GRANT NUMBER(s) ✓ AFOSR-74-2730 ✓
9. PERFORMING ORGANIZATION NAME AND ADDRESS MASSACHUSETTS INSTITUTE OF TECHNOLOGY DEPARTMENT OF AERONAUTICS & ASTRONAUTICS CAMBRIDGE, MA 02139		10. PROGRAM ELEMENT, PROJECT, TASK AREA & WORK UNIT NUMBERS (16) 2307A2 (12) A2 61102F
11. CONTROLLING OFFICE NAME AND ADDRESS AIR FORCE OFFICE OF SCIENTIFIC RESEARCH/NA BLDG 410 BOLLING AIR FORCE BASE, D C 20332		12. REPORT DATE (11) 1978 13. NUMBER OF PAGES 25
14. MONITORING AGENCY NAME & ADDRESS(if different from Controlling Office) (12) 27p.		15. SECURITY CLASS. (of this report) UNCLASSIFIED 15a. DECLASSIFICATION/DOWNGRADING SCHEDULE

16. DISTRIBUTION STATEMENT (of this Report)

Approved for public release; distribution unlimited.

17. DISTRIBUTION STATEMENT (of the abstract entered in Block 20, if different from Report)

18. SUPPLEMENTARY NOTES

19. KEY WORDS (Continue on reverse side if necessary and identify by block number)

TURBULENCE
TURBULENT BURSTING
BOUNDARY LAYER DYNAMICS
COHERENT STRUCTURES

20. ABSTRACT (Continue on reverse side if necessary and identify by block number)

The large-scale coherent motion associated with turbulent bursting in a boundary layer is studied with the aid of an inviscid model. The space-time evolution of a disturbance of large horizontal dimensions compared to the wall layer thickness is analyzed under the assumption that the mean flow is parallel. The initial velocity field is assumed to be set up by the action of the turbulent stresses produced by a patch of secondary instability. For short and moderate times, the effects of viscosity and pressure are small, and the evolution of the disturbance is conveniently studied with the aid of Lagrangian techniques. The model is able to reproduce qualitatively many of the observed features of the bursting

DD FORM 1 JAN 73 1473 EDITION OF 1 NOV 65 IS OBSOLETE

220 003

UNCLASSIFIED

SECURITY CLASSIFICATION OF THIS PAGE (When Data Entered)

LB Grant Page

motion such as the formation of longitudinal streaks, the rapid acceleration after initiation of bursting, and the strong y-coherence of the u-fluctuations. In particular, the model demonstrates how action by the mean shear makes the disturbance eventually evolve into a thin internal shear layer, thus making possible the appearance of a new region of inflexional instability and hence burst regeneration-downstream of the original burst.